European Journal of Neuroscience

WILEY | FENS Federation of European Neuroscience Societies

RESEARCH REPORT

Frequency-Tagging Captures Distinct Neural Responses Elicited by Bilateral Periodic Thermonociceptive Stimulation

Chiara Leu[1,2] | Gabrielle Herbillon[1] | Giulia Liberati[1,3] | Valéry Legrain[1,3,4]

[1]Institute of Neuroscience, Université Catholique de Louvain, Brussels, Belgium | [2]Center for Interdisciplinary Pain Medicine, Department of Neurology and TUM-Neuroimaging Center, School of Medicine and Health, Technical University of Munich, Munich, Germany | [3]Psychological Sciences Research Institute, Université Catholique de Louvain, Louvain-la-Neuve, Belgium | [4]Louvain Bionics, Université Catholique de Louvain, Louvain-la-Neuve, Belgium

Correspondence: Chiara Leu (chiara.leu@uclouvain.be)

Received: 29 October 2025 | **Revised:** 7 April 2026 | **Accepted:** 24 April 2026

Associate Editor: Edmund Lalor

Keywords: intermodulation | pain | steady-state evoked potential (SSEP) | thermonociception

ABSTRACT

Sustained periodic stimuli are known to elicit a periodic neural response (i.e., steady-state evoked potential) in the EEG frequency spectrum. These responses can easily be traced at their frequency of stimulation and corresponding harmonics using a frequency-tagging approach. To date, sustained periodic thermonociceptive stimuli have only been used on one extremity (e.g., right volar forearm) at a time. Extending this procedure to sustained stimulation applied concomitantly to distinct limbs would allow us to study the mechanisms of integration or competition between sensory signals from these different body locations. This study demonstrates that slow, sustained, sinusoidal thermonociceptive stimuli, bilaterally applied using two different stimulation frequencies (i.e., f_1, f_2, one on each forearm), elicit two distinct neural periodic responses at the respective frequency of stimulation and their harmonics. Additionally, we showed preliminary evidence for an interaction between the neural populations involved in the response to these stimuli, marked by neural activity at intermodulation frequencies ($n^* f_1 \pm m^* f_2$). While encouraging, further studies designed specifically to tease out these intermodulation responses are needed to corroborate our findings.

1 | Introduction

Sustained periodic stimuli are known to elicit a periodic neural response at the frequency of stimulation and its harmonics (Regan 1989). This frequency-tagging paradigm has been used for years to explore neural mechanisms underlying sensory perception domains such as auditory (e.g., (Geisler 1960; Pantev et al. 1996)), vision (see Rossion et al. (2020) for a comprehensive review), or rhythm perception (Nozaradan et al. 2018; Nozaradan et al. 2011), but has also been extended to tactile (Moungou et al. 2016) and crucially, thermo-nociceptive stimuli (Colon, Legrain, and Mouraux 2012; Colon, Nozaradan, et al. 2012; Mouraux et al. 2011).

Subsequent investigations demonstrated that an ultra-slow sustained periodic sinusoidal thermo-nociceptive stimulation applied at 0.2 Hz leads to improved signal-to-noise ratio (SNR) of the response to the nociceptive stimulation. Moreover, these slow steady-state evoked potentials (SSEPs) reflect predominantly the activation of slowly adapting C-fibers (Colon et al. 2017). Being thus related to the *secondary* burning and lasting sensation of pain as well as being implicated in tissue inflammation (Campbell and

Abbreviations: EEG, electroencephalography; ERP, event-related potential; f_1, frequency of stimulation 1, i.e., 0.25 Hz; f_2, frequency of stimulation 2, i.e., 0.333 Hz; LMM, linear mixed model; NRS, numerical rating scale; OSF, open science framework; SNR, signal-to-noise ratio; SSEP, steady-state evoked potential.

Meyer 1983), these SSEPs could potentially aid in the understanding of the role of C-fibers in pain perception (Iannetti et al. 2008). While this ultra-slow frequency-tagging paradigm has subsequently been used in a number of scalp EEG investigations (Leu et al. 2023; Leu et al. 2025; Leu et al. 2024; Mulders et al. 2020), which further deepened the understanding of these periodic brain responses, they have always been applied to one single body limb at a time (although sometimes concomitant with a stimulus of another sensory modality, e.g., Colon et al. (2014)). However, these applications do not tap into the full potential of this paradigm; given its high SNR generated, this type of slow sustained stimulus is highly suited to tease out otherwise relatively small differences in neural processing and integration of nociceptive stimuli. In particular, the concomitant application of these stimuli at different body sites, for instance bilaterally on both arms, would also allow us to assess characteristics of cognitive processing induced by, for example, spatial attention tasks (as demonstrated in other sensory modalities (Colon et al. 2015; Giabbiconi et al. 2007; Porcu et al. 2013; Saupe et al. 2009; Toffanin et al. 2009)).

Concomitantly applied sensory periodic stimuli can elicit phenomena known as intermodulation (within the same sensory modality) or cross-modulation (between sensory modalities). Intermodulation refers to a specific frequency-domain manifestation of nonlinear integration, which is defined as a combined neural response to multiple inputs that cannot be accounted for by a linear superposition of the responses to each input presented in isolation. This phenomenon can be observed in the EEG frequency spectrum as neural responses at frequencies corresponding to linear combinations of the stimulation frequencies (i.e., $n*f_1 \pm m*f_2$) (Regan and Regan 1988a; Regan and Regan 1988b; Yang et al. 2016). While audiovisual cross-modulation at these specific frequencies was initially reported (Regan et al. 1995), subsequent studies have failed to replicate this effect using concomitant audiovisual (Giani et al. 2012), visual-tactile (Colon et al. 2015), or nociceptive-visual and nociceptive-tactile stimuli (Colon et al. 2014). Conversely, intermodulation by integration of different streams of visual input has been frequently achieved (reviewed in Chen et al. (2024); Gordon et al. (2019); Xu et al. (2022)). Using vibrotactile stimulation, intermodulation has also been found for concomitant stimulation on the same hand, but not when both hands were stimulated (Pang and Mueller 2015). However, to the best of our knowledge, intermodulation has never been evidenced following concomitant sustained periodic nociceptive stimulation.

Thus, the main aim of this investigation was to demonstrate that the bilateral and concomitant application of ultra-slow sustained periodic sinusoidal thermo-nociceptive stimulation at two different frequencies (f_1, f_2) would elicit a periodic response in the EEG frequency spectrum for both stimulation frequencies. Upon confirmation of this effect, we aimed to further explore the possibility of intermodulation (i.e., nonlinear integration of the concomitant stimuli), a response which would emerge at intermodulation frequencies, a combination of harmonics of f_1 and f_2 (i.e., $n*f_1 \pm m*f_2$).

2 | Methods

This experiment was preregistered on the Open Science Framework (OSF, 10.17605/OSF.IO/KN5QE) prior to the beginning of data collection.

2.1 | Participants

Twenty healthy participants (between 18 and 35 years old) were recruited via an established website and received compensation of 15€ for their participation in the experiment (duration approximately 1.5 h). The data of two participants had to be removed from the analysis due to technical problems with the EEG recordings and were subsequently also removed from the behavioral data analysis. The remaining participants ($n = 18$) were 24.2 ± 3.5 (mean ± std dev) years old (range: 20–35) and eight participants were female. Only right-handed participants were included in the investigation to avoid any potential confound of handedness of the participants in our results.

Exclusion criteria included regular use of psychotropic medication, intake of 1st level analgesics (i.e., paracetamol and nonsteroidal anti-inflammatory drugs) within 12 h before the experiment, as well as any severe neurological diseases, psychiatric disorders, recent trauma, or skin disease affecting upper limbs. All participants gave written informed consent prior to the beginning of the assessment and were informed that they could withdraw from the experiment at any given time. All procedures were performed in accordance with the relevant guidelines and regulations. The local research ethics committee approved all experimental procedures (Commission d'Ethique hospitalo-facultaire Saint-Luc UCLouvain, B403201316436).

The software G*Power was used to conduct a power analysis. We aimed to reach a power of 0.8 using a standard 0.05 alpha error probability. Based on data of Colon et al. (2017), we expected a relatively large effect size ($d = 1.15$) for the detection of a periodic response (tested against zero, one-sided) at the frequency of stimulation, resulting in a suggestion of 10 participants. To account for a potentially smaller effect size given the concomitant bilateral stimulation (as opposed to the commonly used unilateral 0.2 Hz stimulation), to match investigations in other domains, which observed responses at the intermodulation frequencies (Boremanse et al. 2013; Giani et al. 2012) and to account for potential dropouts, we increased the sample size to 20 participants.

2.2 | Stimuli and Materials

Two thermal cutaneous stimulators (TCS II with T03 probe, QST. Lab, Strasbourg, France) were used to deliver sustained periodic thermonociceptive stimuli on the volar forearms of the participants. The probes were set with 15 micro-Peltier elements (each ~7.7 mm^2, arranged in a 30-mm diameter circle), whose temperature can vary at rates of up to 300°C/s. The temperature of stimulation varied between 35°C and 50°C in a sustained periodic sinusoidal manner. Two frequencies of stimulation were applied for 60 s per trial, one on each arm of the participant: Stimulation at frequency 1 (f_1) was delivered at 0.25 Hz (i.e., containing 15 cycles of 4 s), while stimulation at frequency 2 (f_2) was delivered at 0.333 Hz (i.e., containing 20 cycles of 3 s) (Figure 1). The forearm on which f_1 and f_2 were applied was counterbalanced during the experiment, so that the left and right arm received the same number of stimuli with both stimulation frequencies across the experiment. Intertrial intervals were variable and self-paced by the experimenter to allow participants to provide ratings of intensity and

painfulness. The thermodes were displaced after each trial to avoid habituation or sensitization. Stimulation frequencies were determined based on previous studies demonstrating that ultra-slow sustained periodic thermonociceptive stimuli have a superior SNR in frequency-tagging paradigms compared to faster paced thermonociceptive stimulation (Colon et al. 2017). Additionally, the frequencies were chosen so that their harmonics would not overlap in the frequency spectrum. Lastly, we aimed to have stimulation frequencies that are not too different from each other to avoid delivering significantly more stimulation cycles on one arm than on the other during the same trial (i.e., avoiding confounds due to, e.g., difference in terms of temporal summation).

2.3 | Procedure

Participants were seated comfortably in a chair in front of a table, on which both their forearms were resting with the volar surface upwards. They were instructed to move as little as possible and keep their gaze constant to avoid interference with the EEG signal acquisition during the thermonociceptive stimulation. Additionally, they were encouraged to focus their attention on the bilaterally applied stimulation during the trials, that is, on both arms at the same time and not on one arm specifically. In total, 30 trials of the bilateral thermonociceptive stimulation were delivered, split into six blocks of five stimulation trials. The arm on which f_1 and f_2 were applied was randomized and counterbalanced across blocks, so that each arm received an equal amount of stimulation using f_1 and f_2.

2.4 | Behavioral Data

Participants were asked to give a global rating of the intensity of their perception of the bilateral thermonociceptive stimulation on a numerical rating scale (NRS) ranging from 0 ("no perception") to 10 ("most intense perception imaginable") after each trial. Participants were encouraged to give a spontaneous rating, reflecting their perception as adequately as possible. Additionally, they were asked after each trial to evaluate whether they perceived the stimulation as painful, answering either with "yes" or "no." Finally, after each block (i.e., 5 trials), participants were asked whether they perceived the left and right stimulation differently from each other. Prior work from our lab indicates that thermonociceptive SSEPs are largely independent of subjective intensity ratings (Leu et al. 2023, 2024), suggesting that interindividual and intraindividual variability in intensity perception is unlikely to have substantially influenced SSEP amplitudes in the present study. Accordingly, behavioral ratings were recorded primarily to contextualize stimulus perception rather than explain EEG responses.

2.5 | EEG Data

EEG signals were recorded using an elastic electrode-cap with 64 active, preamplified Ag-AgCl electrodes arranged according to the international 10–10 system; signals were digitalized at 1024 Hz and stored for offline analyses (ActiveTwo, BioSemi, the Netherlands). To maintain a clear signal, the direct-current offset was limited to 30 mV. All electrodes were rereferenced offline to the average electrode activity.

The EEG recordings were preprocessed using the Letswave7 (www.letswave.org) toolbox and analyzed using custom scripts in MATLAB 2022a (The MathWorks Inc., Natick, Massachusetts, USA).

2.5.1 | Preprocessing

To process EEG data, we employed a frequency-tagging analysis approach (Regan 1966, 1989) to analyze the periodic response induced by the slow sustained periodic stimuli, which allows for an objective differentiation between oscillatory activity related to the applied stimuli and other unrelated ongoing activity (Colon, Nozaradan, et al. 2012b). The frequency-tagging method is based on the notion that a periodic stimulus elicits a periodic

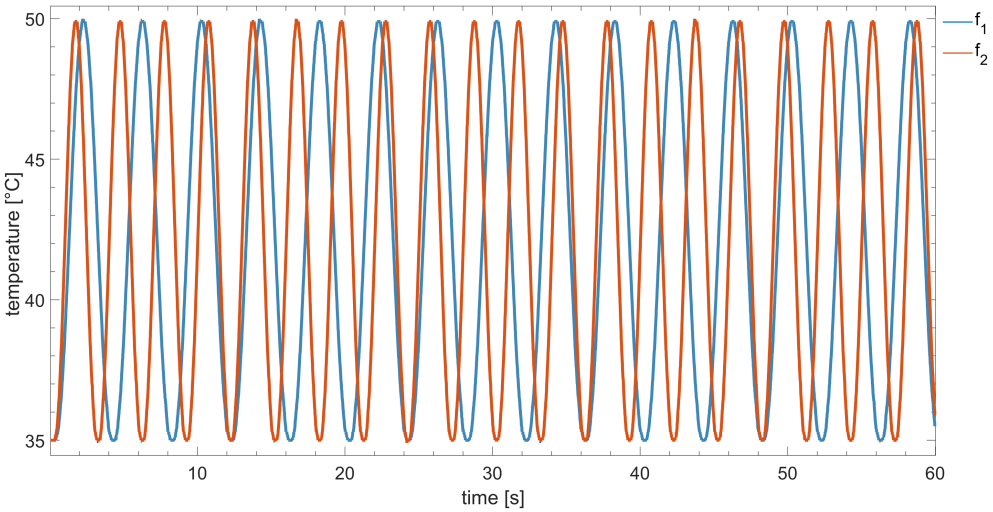

FIGURE 1 | Illustration of the bilateral and concomitant stimulation. Sustained periodic sinusoidal thermonociceptive stimuli were delivered at the frequencies f_1 (0.25 Hz) and f_2 (0.333 Hz), using a thermal cutaneous stimulator (TCS II, QST. Lab, Strasbourg, France).

activity which can be identified as periodic responses at the frequency of stimulation in the recorded EEG signals (Colon, Legrain, and Mouraux 2012; Mouraux et al. 2011). This approach has been frequently used in our lab, leading to a standardized analysis approach (Colon et al. 2017; Leu et al. 2023, 2025, 2024; Mulders et al. 2020).

The obtained EEG signal was first filtered using a fourth-order Butterworth band-pass filter between 0.05 Hz (to remove slow drifts in the recording) and 100 Hz (removing signal outside of our range of interest), then a Notch filter with a 2 Hz width was applied at 50 and 100 Hz. The signal was segmented into epochs of the length of stimulation (60 s), relative to the onset of the stimuli. Because of their placement on the EEG cap, electrodes Iz, P9, and P10 are often very noisy and were therefore removed from the data set to improve signal quality. To remove potential muscular artefacts (i.e., from eye movements), an Independent Component Analysis (Fast ICA algorithm) (Hyvarinen and Oja 2000) was applied, and any trial containing amplitudes larger than 500 μV (peak-to-peak) was removed. On average, ~ 3 ± 2 independent components supposed to reflect noise signals were removed per participant. Less than 1% of trials were removed overall due to large artefacts that could not be removed using the ICA. Noisy channels were interpolated using their three neighboring electrodes. The remaining signal was rereferenced to the average of the electrode set and epochs were concatenated to a length of 120 s, to improve the signal resolution in the frequency domain (frequency resolution = 1/epoch duration, i.e., 1/120 s = 0.00833 Hz). The epochs were then averaged across trials for each participant separately. To analyze the signal in the frequency domain, a discrete Fourier transform (FFT) (Frigo and Johnson 1998) was used. Finally, residual noise was partially removed by subtracting the average amplitude of the signal measured at two to eight neighboring frequencies (thereby excluding the bins immediately adjacent to the bin of interest), at each electrode and at each frequency bin (Mouraux et al. 2011).

2.5.2 | Aggregation of Harmonics

The neural response to periodic stimulation is known to be distributed across harmonics in the frequency spectrum, and these harmonics should be aggregated (i.e., summed up) for an adequate reflection of the neural response to the stimulation (Retter et al. 2021). While there are many different approaches on how to define the ideal number of harmonics to sum, we chose to find the harmonic at which the aggregated signal has the highest signal-to-noise ratio (SNR) in the frequency spectrum, using baseline-corrected group- and channel-averaged data for f_1 and f_2. The SNR was calculated by dividing the signal at a given frequency bin x by the mean amount of noise at the eight surrounding frequency bins (*x/baseline noise*, excluding immediately adjacent bins), providing a stable measure while avoiding overlap with neighboring stimulation frequencies or harmonics. Nevertheless, it cannot be excluded that the overall SNR could be slightly underestimated because of spectral leakage around the bins of interest, despite the removal of the immediately adjacent bin. This method differs slightly from previous investigations from our lab, where the harmonics were either not considered (Colon et al. 2017; Mulders et al. 2020) or all harmonics in the frequency spectrum were aggregated, regardless of their contribution to the SNR (Leu et al. 2023; Leu et al. 2024). Here, we adopted an intermediate approach that retains relevant harmonic components of the brain's response while limiting the inclusion of noise thereby providing a more balanced and reliable estimate of the signal.

To aggregate the harmonics, a custom MATLAB script was used to sum up the amplitude at each harmonic of each frequency of stimulation consecutively and assess the new SNR at each step (evaluated against 8 frequency bins on each side). Based on this evaluation, the highest SNR was identified at 9.25 Hz for f_1 and 7.333 Hz for f_2. Similar to other thermonociceptive SSEP investigations, the first few harmonics carried most of the periodic neural response (Colon et al. 2017; Leu et al. 2023, 2025, 2024; Mulders et al. 2020).

A multi-sensor cluster-based Wilcoxon signed-rank test (clusters built using up to 4 electrode neighbors, 1000 permutations, $p < 0.05$, right-tailed) was used to objectively assess the electrodes with the largest responses (i.e., amplitude) at the aggregated harmonics for f_1 and f_2 separately.

2.5.3 | Intermodulation Responses

To assess intermodulation responses, the baseline-corrected signal was grand averaged across participants and electrodes to avoid a large number of comparisons across frequencies and channels. *Z*-scores were calculated at each frequency bin by calculating the difference between the amplitude of the frequency bin and the averaged amplitude of the 8 frequency bins on each side (16 in total), excluding the immediately adjacent bins, and divided by the standard deviation of these 8 bins (following the formula: x − baseline noise/std $\text{dev}_{\text{baseline noise}}$).

Significant *z*-scores at intermodulation frequencies (i.e., $n^* f_1 \pm m^* f_2$, where n and m are integers, excluding direct harmonics of f_1 and f_2) were identified in the group- and channel-averaged EEG spectrum up to 50 Hz *($p < 0.001$)*. Then, for each channel and participant, the frequency-transformed amplitude was extracted at the frequency bins identified based on the group-level *z*-scores. These chunks (17 bins wide, identified frequency at bin 9) were aggregated to form the "intermodulation response" for each channel and participant. The data were then baseline-corrected and electrodes with activity significantly larger than 0 were identified using the same cluster-based Wilcoxon-signed rank test as described above.

2.5.4 | Assessment of the Number of Trials Necessary for a Good SNR

Finally, a larger number of trials were used in this experiment than in previous frequency-tagging investigations from our lab. To explore how many trials would suffice for a good SNR at the frequency of stimulation and harmonics of f_1 and f_2 (excluding the intermodulation response), we ran the analysis for either the first 6, 12, 18, and 24 trials of each participant and assessed the SNR of the baseline-subtracted group- and channel-averaged signal at the subsequently aggregated harmonics in the frequency spectrum.

2.6 | Statistical Analyses

Statistical analyses were carried out using R Statistical Software (Version 4.3.1, R Core Team 2023) and MATLAB (2022a). The significance level was set at $p \leq 0.001$ for the identification of significant intermodulation responses; consequently, z-scores ≥ 3.1 were considered as significant (one-sided, signal > noise). For other statistical tests, the significance level was set to $p \leq 0.05$.

Linear mixed models (LMMs) including *subject* as random effect (accounting for intercept variations between individuals) were used to assess differences in intensity ratings across the stimulation blocks. A generalized linear mixed effects model with *subject* as random intercept and a binomial error distribution was used to assess the binary ratings of pain perception, testing overall block effects with a Wald χ^2 test. All pairwise comparisons versus block 1 were obtained from model-estimated marginal means with Holm-adjusted p values. A Wilcoxon two-sample paired signed-rank test was used to evaluate whether the aggregated amplitudes elicited by stimulation with f_1 and f_2 differed from each other.

3 | Results

3.1 | Behavioral Data

On average, the stimuli were perceived as painful in 35% of the trials (Figure 2A). Five participants never perceived the stimulation as painful, while for most other participants the number of trials that were perceived as painful varied between the stimulation blocks. The mixed-effects logistic regression did not indicate a significant main effect of stimulation block on whether stimuli were perceived as painful ($\chi^2(5) = 9.260$, $p = 0.099$, $\eta^2 = 0.0103$). All participants indicated that they perceived the stimuli at a similar intensity on both arms. Overall, the stimuli were evaluated at an intensity of 5.33 ± 2.28 (mean ± std dev). A significant main effect of stimulation block was found in the LMM ($F(5, 517) = 3.722$, $p = 0.003$, $\eta^2_p = 0.03$). Post hoc comparisons of model estimated marginal means (EMMs) showed that compared to block 1, mean intensity ratings did not differ significantly in block 2 (EMM = 0.26, 95% CI [−0.18, 0.71], $p = 0.130$, $\eta^2_p = 0.013$) or block 3 (EMM = 0.36, 95% CI [−0.08, 0.81], $p = 0.073$, $\eta^2_p = 0.024$). However, intensity perception ratings were significantly higher in block 4 (EMM = 0.55, 95% CI [0.10, 1.00], $p = 0.005$, $\eta^2_p = 0.054$), block 5 (EMM = 0.58, 95% CI [0.14, 1.03], $p = 0.003$, $\eta^2_p = 0.060$), and block 6 (EMM = 0.60, 95% CI [0.15, 1.05], $p = 0.003$, $\eta^2_p = 0.063$).

3.2 | EEG Data

Stimuli applied with frequency f_1 and f_2 elicited clear periodic responses at their respective frequency of stimulation and their harmonics (Figure 3). The first few harmonics were the largest for both stimulation frequencies, but they were distributed slightly differently across the frequency spectrum, leading to a different number of harmonics that were aggregated to achieve the highest SNR for the response to each stimulation intensity.

The aggregated harmonics demonstrated activity mainly distributed around the scalp vertex (f_1: Z (Cz) = 3.40, $\eta^2_p = 0.640$; f_2: Z (Cz) = 3.57, $\eta^2_p = 0.706$) at both frequencies of stimulation (Figure 3B) as well as at temporal channels in f_1 (Z (TP7) = 3.70, $\eta^2_p = 0.761$; Z (T8) = 3.48, $\eta^2_p = 0.673$). The aggregated amplitudes at the scalp vertex elicited by stimulation with f_1 were

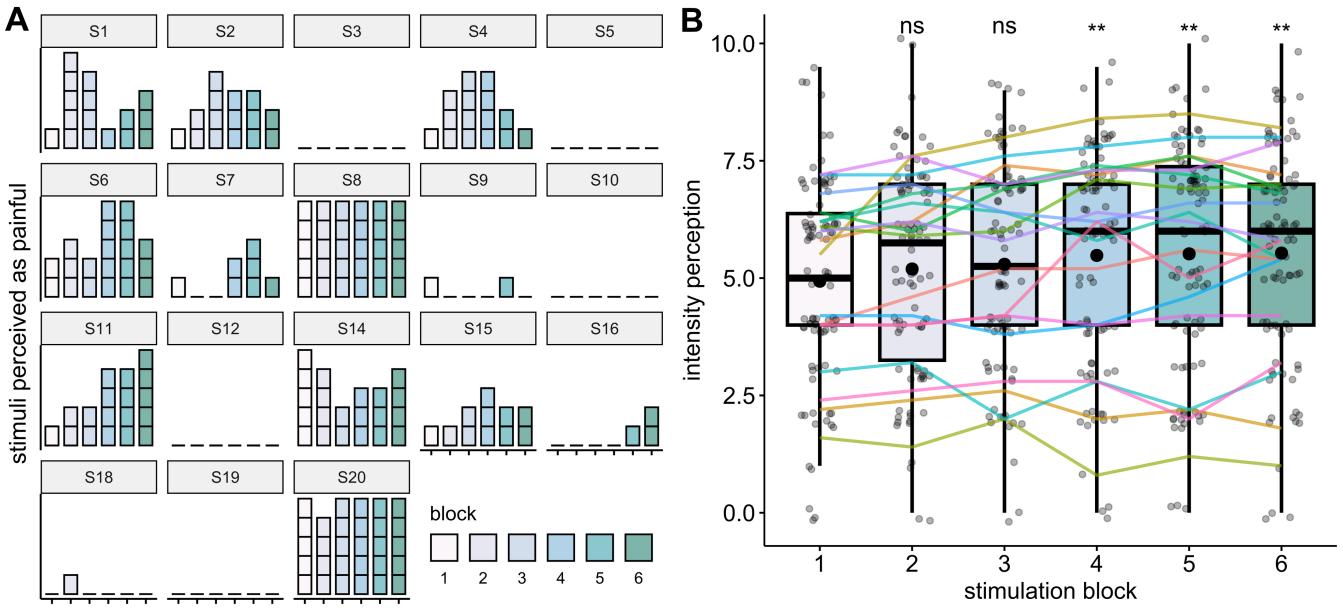

FIGURE 2 | Ratings of perceived painfulness and intensity of the heat pain stimuli. (A) Illustration of the number of trials that were perceived as painful for each participant and each stimulation block. (B) Ratings of perceived stimulation intensity in each block. Horizontal lines indicate the evolution of each participants' average rating per block, while the mean for each block is indicated using round black dots. Individual data points (i.e., data for each trial and each participant) are jittered around the boxplots in grey. Results of the post hoc comparison of the model estimated marginal means comparing each block to block 1 are indicated: $^{ns}p > 0.05$, $^{**}p < 0.01$.

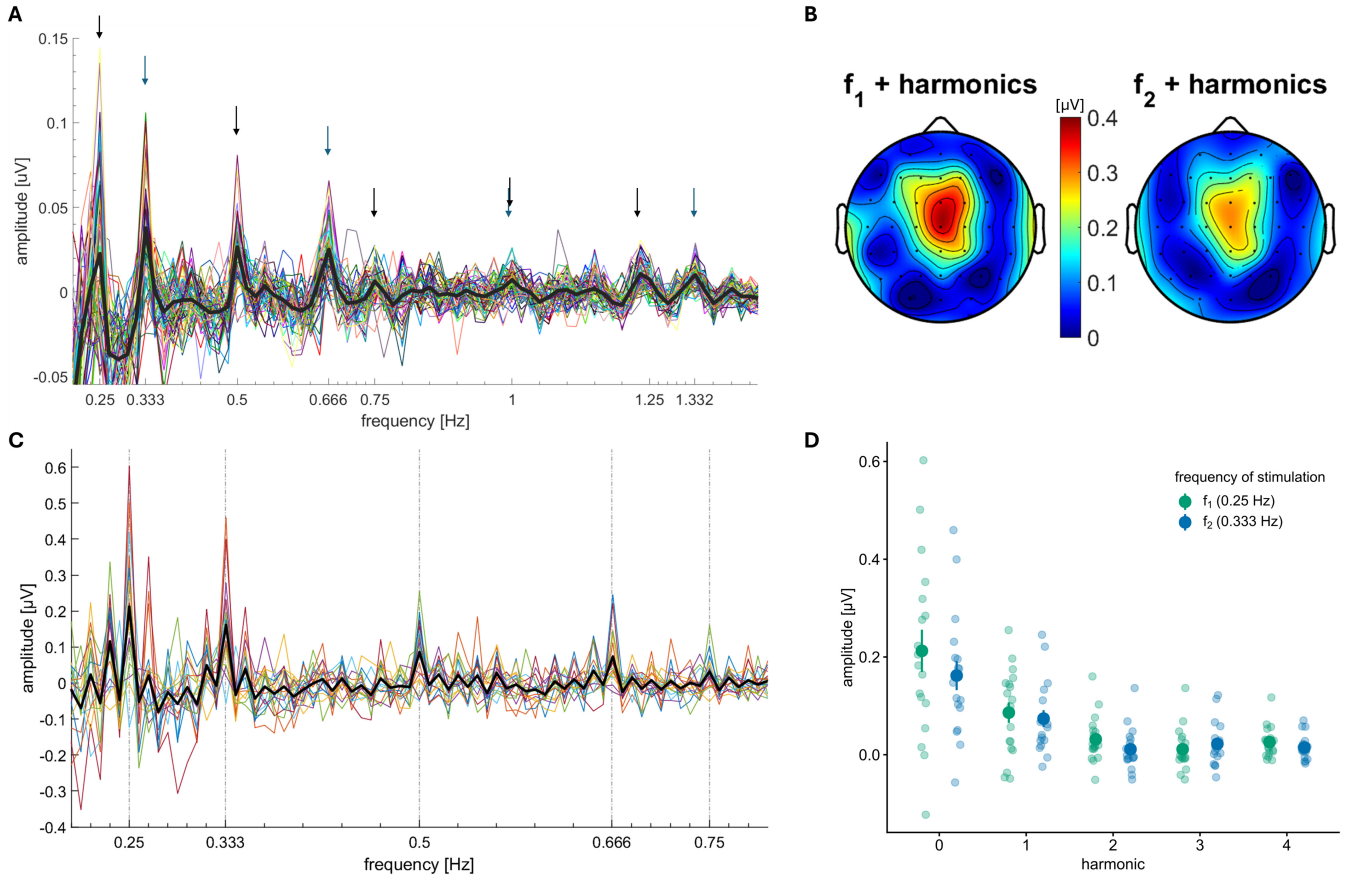

FIGURE 3 | Neural response recorded following concomitant and bilaterally applied sustained periodic thermonociceptive stimulation on the volar forearms. (A) Steady-state evoked potentials elicited by stimuli at frequency f_1 (0.25) and f_2 (0.333) in the EEG frequency spectrum. Group averaged data are indicated for each channel (colored) and the pooled channels (black). (B) Topographical plots represent the response at the aggregated harmonics for f_1 and f_2, based on the number of aggregated harmonics with the highest SNR in the frequency spectrum estimated from group- and channel-averaged data for f_1 and f_2. (C) Responses at channel Cz of each participant (colored) as well as the group-average (black). Reponses at the frequency of stimulation and harmonics are indicated with vertical lines. (D) Subject-level data for the first four harmonics at channel Cz, corresponding to panel C. Group mean and confidence intervals (0.95) are indicated.

slightly larger than the ones elicited by f_2 ($W = 138$, $p = 0.021$, $n = 18$, $\eta^2_p = 0.292$).

As we used a rather large number of trials in this experiment, we also explored how many trials would suffice to achieve a good SNR, having in mind that future studies will likely employ multiple experimental conditions while using bilateral stimuli. This subanalysis on the first 6, 12, 18, and 24 trials of the experiment revealed that at least 12 trials are required to obtain a comparatively good SNR for stimuli at f_1. Interestingly, stimulation frequency f_2 seems to have overall a higher absolute SNR if more than 18 trials are included. The SNR of 12 trials is similar to f_1 with the same number of trials (Figure 4).

Significant intermodulation responses were identified based on z-scored group- and channel-averaged data (Figure 5A). These baseline-corrected responses were aggregated for each channel (Figure 5B), demonstrating a visually identifiable peak at the aggregated intermodulation frequency for most channels. Significant clusters of neural activity were subsequently identified at fronto-central and parietal electrodes (Figure 5C).

4 | Discussion

4.1 | Bilateral Frequency-Tagging of Sustained Periodic Thermonociceptive Stimuli

This proof-of-concept study aimed to demonstrate that bilateral and concomitant application of ultra-slow sustained periodic sinusoidal thermonociceptive stimulation at frequencies f_1 and f_2 elicits periodic neural responses (i.e., SSEPs) at each respective frequency of stimulation (and its harmonics), which can objectively identified using a frequency-tagging approach. Additionally, we investigated whether the simultaneous activation of potentially similar neuronal populations by the bilateral stimulation leads to a nonlinear integration of the nociceptive input, which would be present at intermodulation frequencies (i.e., $n^* f_1 \pm m^* f_2$).

Both stimuli elicited clear SSEPs in the frequency spectrum at the frequency of stimulation and their harmonics. The largest periodic response to these concomitantly applied ultra-slow stimuli was found at the scalp vertex for both stimuli, consistent with other thermonociceptive SSEP investigations (Colon et al. 2017; Leu et al. 2023, 2025, 2024; Mulders et al. 2020), The obtained frequency spectra further parallel the previous

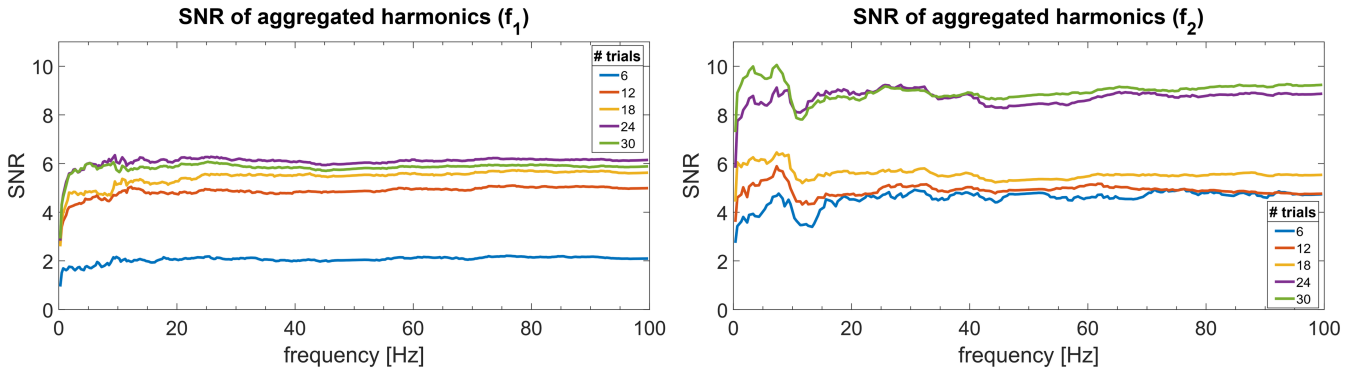

FIGURE 4 | SNR development across the frequency spectrum for different numbers of trials. For each frequency of stimulation, the number of trials averaged before the frequency transformation was gradually decreased to assess its impact on the SNR across the frequency spectrum. The aim was to find the lowest number of trials still achieving a comparatively high SNR.

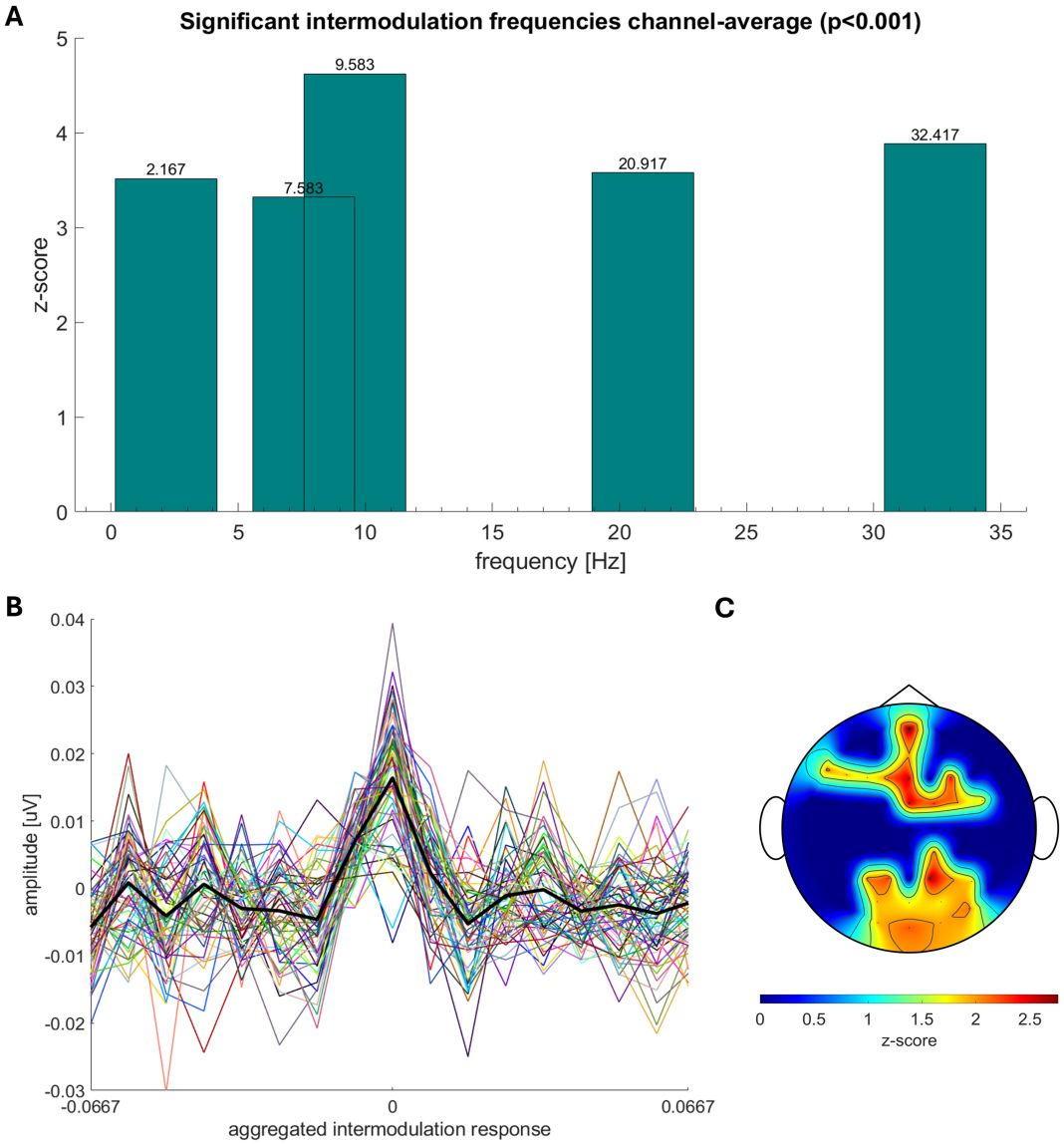

FIGURE 5 | Neural activity at intermodulation frequencies. (A) Intermodulation frequencies of the group- and channel-averaged response that exhibited an amplitude with a z-score > 3.1. (B) Baseline-corrected and group-averaged activity of all channels at the aggregated intermodulation frequency. The black line marks the average of all channels. (C) Representation of electrodes exhibiting a response significantly larger than 0 (following a cluster-based Wilcoxon signed-rank test) in the aggregated intermodulation response.

thermonociceptive SSEP investigations, as the first few harmonics carried most of the periodic neural response. While the magnitude of the aggregated response differed slightly between f_1 and f_2, this is likely due to the relatively large difference in the number of harmonics that were aggregated in each response.

Previous studies comparing time-locked event-related potentials (ERPs) elicited by bilateral vs. unilateral application of brief thermonociceptive laser stimuli reported inconsistent results. In one experiment, ERP magnitudes elicited by bilateral stimulation decreased compared to unilateral stimulation (Northon et al. 2018), while they increased (particularly when the hands were close to the body) in another (Northon et al. 2022). One reason for the variability in these results may be that, because ERPs are obtained by averaging EEG signals in the time domain and therefore reflect superposition of the different responses indiscriminately, this does not allow for understanding the individual contribution of the ascending signals generated by each limb stimulation. Using a SSEP paradigm with two distinct stimulation frequencies could address this, allowing for clearer differentiation of input from each stimulated arm. Future studies could directly compare unilateral and bilateral stimulation to better understand how the brain processes concomitant versus single streams of thermonociceptive stimulation.

Given the relatively large number of trials in this experiment, we examined how reducing trial count would affect the SNR at the frequencies of stimulation and their harmonics. This is particularly relevant for future studies, where multiple conditions make high trial numbers impractical due to participant discomfort and long sessions. Our analysis showed that fewer than 30 trials were sufficient, with at least 12 trials providing good SNR at both frequencies, consistent with similar unilateral thermonociceptive stimulation studies.

Another reason to reduce the number of trials is the observed increase in stimulus intensity ratings over the course of the experiment, with significantly higher ratings in blocks 4–6 compared to block 1. This increase is likely related to the phenomenon of peripheral sensitization. Although the location of the thermode was shifted after each stimulus, given the total number of 30 stimuli, repeated stimulation of nearby areas with the same stimulation was unavoidable, potentially leading to spatial summation (Nielsen and Arendt-Nielsen 1997). This observed sensitization emphasizes the need to limit the number of stimuli in future SSEP studies using ultra-slow sustained periodic thermonociceptive stimulation. Curiously, the number of trials perceived as painful is about half of the percentage of trials reported as painful in previous investigations (Leu et al. 2023, 2024), despite similar levels of intensity perception. The repetitive and predictive nature of the applied stimuli might have contributed to a decrease in the level of *perceived bodily threat* of these stimuli. In the previously mentioned thermonociceptive SSEP investigations, variations in conditions were always present; therefore, leading to more variations in perception and potentially reducing the predictability of the stimuli.

A limitation of this experiment is that the chosen frequencies of stimulation are challenging to assess in the frequency spectrum due to the characteristics of frequency f_2 (i.e., frequency of 0.333 Hz). The resolution in the frequency domain is limited by the duration of the trial; thus, a stimulation frequency with a higher precision than the frequency resolution is likely to succumb to rounding errors, as harmonics may fall into adjacent frequency bins rather than precisely where expected. This makes it more difficult to identify the exact responses to the applied stimuli, particularly when trying to aggregate harmonic responses. These frequencies were nevertheless selected based on experimental considerations related to participant perception. Specifically, the use of two close but nonidentical stimulation frequencies (0.25 and 0.333 Hz) was intended to reduce temporal predictability of the stimulation while ensuring comparable stimulation rates across arms. An improvement for future investigations would be to use a similarly slow frequency of stimulation with a more convenient value, for example, 0.4 Hz, so that harmonics align more precisely with frequency bins and can be analyzed more reliably.

4.2 | Intermodulation

A key difference from earlier studies on nonlinear nociceptive integration may be the improved SNR achieved with ultra-slow stimulation (Colon et al. 2017). Previous work using faster (> 3 Hz) thermonociceptive or low-intensity intraepidermal electrical stimuli primarily activated Aδ-fibers and yielded relatively low SNR (Colon, Nozaradan, et al. 2012b), limiting sensitivity to potential cross-modal effects as observed in (Colon et al. 2014). The enhanced SNR obtained with ultra-slow stimulation might therefore provide a more suitable approach to re-examining sensory integration. This rationale also motivated us to revisit potential intermodulation effects within the nociceptive modality as an additional exploratory analysis in the present study.

With the successful implementation of the bilateral frequency-tagging using thermonociceptive stimuli, we set out to identify significant responses at intermodulation frequencies, which could illustrate the nonlinear neural integration of the concomitantly applied stimuli. Because the neural activity elicited by these stimuli was most prominent at the scalp vertex, we expected that their activity might *overlap* and create an interaction, leading to the neural integration of the input of the two applied stimuli. This hypothesis was also supported by the perception of the participants, which—while not necessarily being perceived *as one*—also did not differ between the stimuli. This could have also been facilitated by the use of a global perception rating, rather than asking participants for a separate rating for each arm. Using a standard z-score threshold, we found a number of significant z-scored frequency bins across the frequency spectrum in the grand-averaged and channel-pooled data. Thus, to be more selective and forego issues of multiple comparison, we increased the significance threshold to a more conservative $p < 0.001$. Still, multiple amplitudes exceeded this threshold.

The phenomenon of intermodulation following concomitant and periodic sensory input is not new. In the visual domain, the usefulness of neural integration of two different stimuli has elegantly been demonstrated by periodically presenting half-faces at different frequencies, during which the brain tries to integrate the information to a complete face (Boremanse et al. 2013, 2014). Comparatively, it is less clear what the responses recorded at intermodulation frequencies reflect in the context of

bilateral thermonociceptive stimulation. Usually, intermodulation frequencies can be found only few harmonic combinations away from their "base" frequency (e.g., $1*f_1 + 1*f_2$). This was not the case in this investigation, where intermodulation frequencies were identified predominantly at higher harmonic combinations, which raises the question of what processes these responses reflect. As slow stimulation frequencies can lead to relevant harmonics being more spread out throughout the spectrum (Retter et al. 2021), shifting responses at intermodulation frequencies to appear at later harmonics. Nevertheless, the fact that no intermodulation responses were found at early harmonic combinations in the *z*-scored signal indicates that these responses were relatively small. This could have been partially caused by the timing of the two stimuli, which were never truly simultaneous (i.e., the applied heat cycles never reached their maximum exactly at the same time, though close to each other) and peaked sometimes relatively far from each other, which could have hampered a potential cleaner neural integration output. In an exploratory analysis, we isolated stimulation cycles that peaked almost simultaneously (see Figure 1, first cycle of the stimulation) and analyzed only this portion of the signal. While this exploratory analysis led to identifiable peaks at the first intermodulation frequency, we cannot be certain that the correct f_2 frequency was identified, as aligning cycles to f_1 disrupted the regularity of f_2 in the time domain, potentially splitting it into two frequencies after transformation. We should thus not consider this analysis as definitive evidence for a present but "hidden" intermodulation effect within our data. Moreover, it should be considered that 0.333 Hz does not align precisely with the discrete Fourier frequency bins. This bin mismatch may have caused spectral leakage or slight shifts of potential intermodulation components into adjacent bins, thereby reducing sensitivity and possibly rendering such responses undetectable in the applied frequency-tagging analysis. Because the intermodulation analysis was exploratory and conceived after data acquisition, we were unable to optimize the frequency selection; future studies should therefore employ stimulation frequencies that align clearly with frequency bins to allow more conclusive assessment of intermodulation effects. Thus, while these higher harmonic responses could reflect intermodulation as the brain integrates sensory input from each arm within a distinct neural population, their small size at unusually high harmonics warrants a cautious interpretation. The observed responses might also relate to other, network-level interactions such as interhemispheric coupling (i.e., the functional interaction between homologous cortical regions). The synchronization of oscillatory activity between the somatosensory cortices in both hemispheres could lead to phase/amplitude coupling (Bloom and Hynd 2005) and thus potentially to responses at intermodulation frequencies which are not strictly related to a nonlinear sensory integration within one neural population. While attentional processes could also contribute to the observed effects, evidence from our lab indicates that frequency-tagged responses to sustained thermonociceptive stimulation are not strongly modulated by attention manipulations (Leu et al. 2023, 2025), making this explanation less likely. Nevertheless, disentangling the precise underlying mechanisms warrants a dedicated and well-controlled experiment, focusing in particular on the distinction between computational nonlinear integration and network-level interactions. Although the present study cannot resolve the issue conclusively, our findings provide a foundation for future research investigating how the human brain integrates concomitant thermonociceptive activation, either in isolation or in combination with other sensory modalities.

5 | Conclusions

This investigation successfully demonstrated that sustained periodic thermonociceptive stimuli applied concomitantly to both forearms at frequencies f_1 and f_2 elicit a periodic neural response at both frequencies of stimulation, easily identifiable using frequency tagging. This paves the way for extending the frequency-tagging paradigm to a bilateral application of (thermo-)nociceptive stimuli, a promising paradigm to better understand the neural representation and integration of concomitant nociceptive stimuli. In an exploratory analysis, we observed periodic responses at intermodulation frequencies. Whether these responses indicate nonlinear integration of the concomitantly applied thermonociceptive stimulation could not be determined conclusively. Nevertheless, these results might encourage further research into whether slow sustained periodic thermonociceptive stimulation could be beneficial not only to better understand nociceptive processing by itself, but also its sensory integration in relation to other sensory stimuli.

Author Contributions

Chiara Leu: conceptualization, data curation, formal analysis, investigation, methodology, software, validation, visualization, writing – original draft, writing – review and editing. **Gabrielle Herbillon:** conceptualization, investigation, methodology, writing – review and editing. **Giulia Liberati:** supervision, writing – review and editing. **Valéry Legrain:** conceptualization, funding acquisition, resources, supervision, writing – review and editing.

Acknowledgements

We wish to thank Francesca Barbero and members of the Pain Research Lab at UCLouvain for their helpful feedback and suggestions. The preprint version of this article is available at 10.1101/2025.07.31.667970.

Funding

C.L., G.H., G.L., and V.L. are supported by the Belgian Fund for Scientific Research of the French-speaking community of Belgium (F.R.S.-FNRS). C.L. is further supported by the Swiss National Science Foundation (P500-3_239275).

Conflicts of Interest

The authors declare no conflicts of interest.

Data Availability Statement

The data that support the findings of this study are openly available in the project repository at OSF (10.17605/OSF.IO/6QTUR).

Peer Review

The peer review history for this article is available at https://www.webofscience.com/api/gateway/wos/peer-review/10.1111/ejn.70539.

References

Bloom, J. S., and G. W. Hynd. 2005. "The Role of the Corpus Callosum in Interhemispheric Transfer of Information: Excitation or Inhibition?" *Neuropsychology Review* 15, no. 2: 59–71. https://doi.org/10.1007/s11065-005-6252-y.

Boremanse, A., A. M. Norcia, and B. Rossion. 2013. "An Objective Signature for Visual Binding of Face Parts in the Human Brain." *Journal of Vision* 13, no. 11: 6. https://doi.org/10.1167/13.11.6.

Boremanse, A., A. M. Norcia, and B. Rossion. 2014. "Dissociation of Part-Based and Integrated Neural Responses to Faces by Means of Electroencephalographic Frequency Tagging." *European Journal of Neuroscience* 40, no. 6: 2987–2997. https://doi.org/10.1111/ejn.12663.

Campbell, J. N., and R. A. Meyer. 1983. "Sensitization of Unmyelinated Nociceptive Afferents in Monkey Varies With Skin Type." *Journal of Neurophysiology* 49, no. 1: 98–110. https://doi.org/10.1152/jn.1983.49.1.98.

Chen, Y., J. Bai, N. Shi, et al. 2024. "Intermodulation Frequency Components in Steady-State Visual Evoked Potentials: Generation, Characteristics and Applications." *NeuroImage* 303: 120937. https://doi.org/10.1016/j.neuroimage.2024.120937.

Colon, E., V. Legrain, G. Huang, and A. Mouraux. 2015. "Frequency Tagging of Steady-State Evoked Potentials to Explore the Crossmodal Links in Spatial Attention Between Vision and Touch." *Psychophysiology* 52, no. 11: 1498–1510. https://doi.org/10.1111/psyp.12511.

Colon, E., V. Legrain, and A. Mouraux. 2012. "Steady-State Evoked Potentials to Study the Processing of Tactile and Nociceptive Somatosensory Input in the Human Brain." *Neurophysiologie Clinique/Clinical Neurophysiology* 42, no. 5: 315–323. https://doi.org/10.1016/j.neucli.2012.05.005.

Colon, E., V. Legrain, and A. Mouraux. 2014. "EEG Frequency Tagging to Dissociate the Cortical Responses to Nociceptive and Nonnociceptive Stimuli." *Journal of Cognitive Neuroscience* 26, no. 10: 2262–2274. https://doi.org/10.1162/jocn_a_00648.

Colon, E., G. Liberati, and A. Mouraux. 2017. "EEG Frequency Tagging Using Ultra-Slow Periodic Heat Stimulation of the Skin Reveals Cortical Activity Specifically Related to C Fiber Thermonociceptors." *NeuroImage* 146: 266–274. https://doi.org/10.1016/j.neuroimage.2016.11.045.

Colon, E., S. Nozaradan, V. Legrain, and A. Mouraux. 2012. "Steady-State Evoked Potentials to Tag Specific Components of Nociceptive Cortical Processing." *NeuroImage* 60, no. 1: 571–581. https://doi.org/10.1016/j.neuroimage.2011.12.015.

Frigo, M., and S. G. Johnson. 1998. "FFTW: An Adaptive Software Architecture for the FFT." Proceedings of the 1998 IEEE International Conference on Acoustics, Speech and Signal Processing, ICASSP '98 (Cat. No.98CH36181).

Geisler, C. D. 1960. "Average Responses to Clicks in Man Recorded by Scalp Electrodes."

Giabbiconi, C. M., N. J. Trujillo-Barreto, T. Gruber, and M. M. Müller. 2007. "Sustained Spatial Attention to Vibration Is Mediated in Primary Somatosensory Cortex." *NeuroImage* 35, no. 1: 255–262. https://doi.org/10.1016/j.neuroimage.2006.11.022.

Giani, A. S., E. Ortiz, P. Belardinelli, M. Kleiner, H. Preissl, and U. Noppeney. 2012. "Steady-State Responses in MEG Demonstrate Information Integration Within but Not Across the Auditory and Visual Senses." *NeuroImage* 60, no. 2: 1478–1489. https://doi.org/10.1016/j.neuroimage.2012.01.114.

Gordon, N., J. Hohwy, M. J. Davidson, J. J. A. van Boxtel, and N. Tsuchiya. 2019. "From Intermodulation Components to Visual Perception and Cognition-A Review." *NeuroImage* 199: 480–494. https://doi.org/10.1016/j.neuroimage.2019.06.008.

Hyvarinen, A., and E. Oja. 2000. "Independent Component Analysis: Algorithms and Applications." *Neural Networks* 13, no. 4–5: 411–430. https://doi.org/10.1016/s0893-6080(00)00026-5.

Iannetti, G. D., N. P. Hughes, M. C. Lee, and A. Mouraux. 2008. "Determinants of Laser-Evoked EEG Responses: Pain Perception or Stimulus Saliency?" *Journal of Neurophysiology* 100, no. 2: 815–828. https://doi.org/10.1152/jn.00097.2008.

Leu, C., A. Courtin, C. Cussac, and G. Liberati. 2023. "The Role of Ongoing Oscillation in Pain Perception: Absence of Modulation by a Concomitant Arithmetic Task." *Cortex* 168: 114–129. https://doi.org/10.1016/j.cortex.2023.08.005.

Leu, C., S. Forest, V. Legrain, and G. Liberati. 2025. "The Effect of Stimulus Saliency on the Modulation of Ongoing Neural Oscillations Related to Thermonociception: A Registered Report." *Cortex* 185: 316–335. https://doi.org/10.1016/j.cortex.2025.02.009.

Leu, C., E. Glineur, and G. Liberati. 2024. "Cue-Based Modulation of Pain Stimulus Expectation: Do Ongoing Oscillations Reflect Changes in Pain Perception? A Registered Report." *Royal Society Open Science* 11, no. 6: 240626. https://doi.org/10.1098/rsos.240626.

Moungou, A., J.-L. Thonnard, and A. Mouraux. 2016. "EEG Frequency Tagging to Explore the Cortical Activity Related to the Tactile Exploration of Natural Textures." *Scientific Reports* 6, no. 1: 20738. https://doi.org/10.1038/srep20738.

Mouraux, A., G. D. Iannetti, E. Colon, S. Nozaradan, V. Legrain, and L. Plaghki. 2011. "Nociceptive Steady-State Evoked Potentials Elicited by Rapid Periodic Thermal Stimulation of Cutaneous Nociceptors." *Journal of Neuroscience* 31, no. 16: 6079–6087. https://doi.org/10.1523/jneurosci.3977-10.2011.

Mulders, D., C. de Bodt, N. Lejeune, et al. 2020. "Dynamics of the Perception and EEG Signals Triggered by Tonic Warm and Cool Stimulation." *PLoS ONE* 15, no. 4: e0231698. https://doi.org/10.1371/journal.pone.0231698.

Nielsen, J., and L. Arendt-Nielsen. 1997. "Spatial Summation of Heat Induced Pain Within and Between Dermatomes." *Somatosensory & Motor Research* 14, no. 2: 119–125. https://doi.org/10.1080/08990229771123.

Northon, S., Z. Deldar, and M. Piché. 2022. "Effects of Spatial Attention and Limb Position on the Cortical Interaction of Bilateral Noxious Inputs." *Psychophysiology* 59, no. 2: e13966. https://doi.org/10.1111/psyp.13966.

Northon, S., N. Rustamov, and M. Piché. 2018. "Cortical Integration of Bilateral Nociceptive Signals: When More Is Less." *Pain* 160, no. 3: 724–733. https://doi.org/10.1097/j.pain.0000000000001451.

Nozaradan, S., P. E. Keller, B. Rossion, and A. Mouraux. 2018. "EEG Frequency-Tagging and Input–Output Comparison in Rhythm Perception." *Brain Topography* 31, no. 2: 153–160. https://doi.org/10.1007/s10548-017-0605-8.

Nozaradan, S., I. Peretz, M. Missal, and A. Mouraux. 2011. "Tagging the Neuronal Entrainment to Beat and Meter." *Journal of Neuroscience* 31, no. 28: 10234–10240. https://doi.org/10.1523/jneurosci.0411-11.2011.

Pang, C. Y., and M. M. Mueller. 2015. "Competitive Interactions in Somatosensory Cortex for Concurrent Vibrotactile Stimulation Between and Within Hands." *Biological Psychology* 110: 91–99. https://doi.org/10.1016/j.biopsycho.2015.07.002.

Pantev, C., L. E. Roberts, T. Elbert, B. Roβ, and C. Wienbruch. 1996. "Tonotopic Organization of the Sources of Human Auditory Steady-State Responses." *Hearing Research* 101, no. 1: 62–74. https://doi.org/10.1016/S0378-5955(96)00133-5.

Porcu, E., C. Keitel, and M. M. Müller. 2013. "Concurrent Visual and Tactile Steady-State Evoked Potentials Index Allocation of Inter-Modal Attention: A Frequency-Tagging Study." *Neuroscience Letters* 556: 113–117. https://doi.org/10.1016/j.neulet.2013.09.068.

Regan, D. 1966. "Some Characteristics of Average Steady-State and Transient Responses Evoked by Modulated Light." *Electroencephalography and Clinical Neurophysiology* 20, no. 3: 238–248. https://doi.org/10.1016/0013-4694(66)90088-5.

Regan, D. 1989. "Human Brain Electrophysiology. Evoked Potentials and Evoked Magnetic Fields in Science and Medicine."

Regan, D., and M. P. Regan. 1988a. "Objective Evidence for Phase-Independent Spatial Frequency Analysis in the Human Visual Pathway." *Vision Research* 28, no. 1: 187–191. https://doi.org/10.1016/S0042-6989(88)80018-X.

Regan, M. P., and D. Regan. 1988b. "A Frequency Domain Technique for Characterizing Nonlinearities in Biological Systems." *Journal of Theoretical Biology* 133, no. 3: 293–317. https://doi.org/10.1016/S0022-5193(88)80323-0.

Regan, M. P., D. Regan, and P. He. 1995. "An Audio-Visual Convergence Area in the Human Brain." *Experimental Brain Research* 106, no. 3: 485–487. https://doi.org/10.1007/BF00231071.

Retter, T. L., B. Rossion, and C. Schiltz. 2021. "Harmonic Amplitude Summation for Frequency-Tagging Analysis." *Journal of Cognitive Neuroscience* 33, no. 11: 2372–2393. https://doi.org/10.1162/jocn_a_01763.

Rossion, B., T. L. Retter, and J. Liu-Shuang. 2020. "Understanding Human Individuation of Unfamiliar Faces With Oddball Fast Periodic Visual Stimulation and Electroencephalography." *European Journal of Neuroscience* 52, no. 10: 4283–4344. https://doi.org/10.1111/ejn.14865.

Saupe, K., E. Schröger, S. K. Andersen, and M. M. Müller. 2009. "Neural Mechanisms of Intermodal Sustained Selective Attention With Concurrently Presented Auditory and Visual Stimuli." *Frontiers in Human Neuroscience* 3: 58. https://doi.org/10.3389/neuro.09.058.2009.

Toffanin, P., R. de Jong, A. Johnson, and S. Martens. 2009. "Using Frequency Tagging to Quantify Attentional Deployment in a Visual Divided Attention Task." *International Journal of Psychophysiology* 72, no. 3: 289–298. https://doi.org/10.1016/j.ijpsycho.2009.01.006.

Xu, S., X. Zhou, and L. Chen. 2022. "Intermodulation From Unisensory to Multisensory Perception: A Review." *Brain Sciences* 12, no. 12: 1617. https://www.mdpi.com/2076-3425/12/12/1617.

Yang, Y., T. Solis-Escalante, F. C. T. van der Helm, and A. C. Schouten. 2016. "A Generalized Coherence Framework for Detecting and Characterizing Nonlinear Interactions in the Nervous System." *IEEE Transactions on Biomedical Engineering* 63, no. 12: 2629–2637. https://doi.org/10.1109/TBME.2016.2585097.